

**Title:** Inhibition of the motor protein Eg5/Kinesin-5 in amyloid beta-mediated impairment of hippocampal long-term potentiation and dendritic spine loss\*

**Authors:** Ronald K. Freund, Emily S. Gibson, Huntington Potter, and Mark L. Dell'Acqua

**Affiliations:**

RKF, ESG, MLD: Department of Pharmacology, University of Colorado School of Medicine, Anschutz Medical Campus, Aurora, CO 80045

HP: Department Neurology, University of Colorado School of Medicine, Anschutz Medical Campus, Aurora, CO 80045

MLD, HP: Linda Crnic Institute for Down Syndrome, University of Colorado, Anschutz Medical Campus, Aurora, CO 80045

**Running Title:** A $\beta$ -mediated Synaptic Dysfunction by Eg5 Inhibition

**Corresponding Authors:**

Ronald K. Freund, Ph.D.  
Dept. of Pharmacology  
University of Colorado School of Medicine  
Anschutz Medical Campus  
12800 E. 19<sup>th</sup> Ave.  
Mail Stop 8303  
Aurora, CO 80045  
Phone: 303-724-3641  
Fax: 303-724-3640  
Email: [ron.freund@ucdenver.edu](mailto:ron.freund@ucdenver.edu)

And

Mark L. Dell'Acqua, Ph.D.  
Dept. of Pharmacology  
University of Colorado School of Medicine  
12800 E. 19<sup>th</sup> Ave.  
Mail Stop 8303  
Aurora, CO 80045  
Phone: 303-724-3616  
Fax: 303-724-3633  
Email: [mark.dellacqua@ucdenver.edu](mailto:mark.dellacqua@ucdenver.edu)

**Text pages:** 28

**Tables:** 0

**Figures:** 5

**References:** 49

**Abstract:** 249 words

**Introduction:** 675 words

**Discussion:** 1496 words

**Abbreviations:**  $\alpha$ -amino-3-hydroxy-5-methyl-4-isoxazolepropionic acid receptor, AMPAR; Alzheimer's disease, AD; (DL)-amino-5-phosphonovaleric acid, APV; amyloid beta, A $\beta$ ; amyloid precursor protein, APP; artificial cerebrospinal fluid, aCSF; day-*in-vitro*, DIV; cornus ammonis 1, CA1; 6-cyano-7-nitroquinoxaline-2,3-dione, CNQX; field excitatory postsynaptic potential, fEPSP; green fluorescent protein, GFP; Long-term potentiation, LTP; N-methyl-D-aspartate receptor, NMDAR.

## Abstract

Alzheimer's Disease (AD) is characterized by neurofibrillary tangles, amyloid plaques and neurodegeneration. However, this pathology is preceded by increased soluble amyloid beta (A $\beta$ ) oligomers that interfere with glutamatergic synaptic plasticity required for learning and memory, including N-methyl-D-aspartate receptor (NMDAR)-dependent long-term potentiation (LTP). In particular, soluble A $\beta$ (1-42) acutely inhibits LTP and chronically causes synapse loss. While many mechanisms are proposed for A $\beta$ -induced synaptic dysfunction, we recently found that A $\beta$ (1-42) inhibits the microtubule motor protein Eg5/Kinesin-5. Here we compared the impacts of A $\beta$ (1-42) and monastrol, a small molecule Eg5 inhibitor, on LTP in hippocampal slices and synapse loss in neuronal cultures. Acute (20 min) treatment with monastrol, like A $\beta$ , completely inhibited LTP at doses >100 nM. In addition, 1 nM A $\beta$ (1-42) or 50 nM monastrol inhibited LTP ~ 50%, and when applied together, caused complete LTP inhibition. At concentrations that impaired LTP, neither A $\beta$ (1-42) nor monastrol inhibited NMDAR synaptic responses until ~60 min, when only ~25% inhibition was seen for monastrol, indicating that NMDAR inhibition was not responsible for LTP inhibition by either agent when applied for only 20 min. Finally, 48 hour treatment with either 0.5-1.0  $\mu$ M A $\beta$ (1-42) or 1-5  $\mu$ M monastrol reduced dendritic spine/synapse density in hippocampal cultures up to a maximum of ~40%, and when applied together at maximal concentrations, no additional spine loss resulted. Thus, monastrol can mimic, and in some cases occlude, the impacts of A $\beta$  on LTP and synapse loss, suggesting that A $\beta$  induces acute and chronic synaptic dysfunction in part through inhibiting Eg5.

## Introduction

Alzheimer's Disease (AD) is a neurodegenerative disease that affects cognition primarily in the elderly. With advances in modern medicine successfully treating other diseases and leading to overall increased lifespan, it is estimated that the number of people with AD will likely exceed 15 million in the US and 50 million worldwide by 2050. However, there are currently no effective treatments for AD, thus it is expected that the already substantial burdens that caring for AD patients places on the US and world economies and health care systems will increase dramatically in the future (Wimo et al., 2011).

The hallmarks of AD include amyloid plaques and neurofibrillary tangles in postmortem brain. Plaques contain insoluble filaments of amyloid beta ( $A\beta$ ) peptides, which arise from proteolytic processing of the amyloid precursor protein (APP), a transmembrane cell-adhesion protein. Similarly, tangles are oligomers of hyper-phosphorylated tau, a microtubule-associated protein. However, plaques, and to a lesser extent tangles, are poor indicators of cognitive impairment in AD, especially in early disease stages prior to extensive tangle formation and plaque deposition (Dickson et al., 1995; Terry et al., 1991). Instead, soluble forms of  $A\beta$  are thought to be largely responsible for driving brain dysfunction in early AD (McLean et al., 1999; Naslund et al., 2000) by interfering with excitatory synaptic function through a variety of mechanisms, including by promoting tau phosphorylation (reviewed in Mucke and Selkoe, 2012).

Accordingly, acute application of synthetic  $A\beta(1-42)$  peptides (Lambert et al., 1998) or  $A\beta$  extracted from AD brains (Shankar et al., 2007; Shankar et al., 2008) can disrupt synaptic plasticity in brain regions that are important for learning and memory, such as inhibiting LTP at hippocampal CA1 synapses. While  $A\beta(1-42)$  monomers do not alter LTP,  $A\beta$  forms low molecular weight, soluble oligomers, including dimers and trimers, that potently inhibit LTP (McLean et al., 1999; Naslund et al., 2000; Selkoe, 2008; Shankar et al., 2007; Shankar et al., 2008; Walsh et al., 2002). Several hypotheses

have been posited to explain how A $\beta$  inhibits LTP and alters brain function through perturbing various signaling pathways. In this regard A $\beta$  can interact with a number of different membrane receptors, including NMDA (Ari et al., 2014; Kurup et al., 2010; Shankar et al., 2007) and metabotropic glutamate receptors (Hsieh et al., 2006; Um et al., 2013),  $\alpha$ 7 nicotinic acetylcholine receptors (Lui et al., 2012; Snyder et al., 2005; Wang et al., 2000a, 2000b), paired immunoglobulin-like receptor B (Kim et al., 2013), cellular prion protein (Lauren et al., 2009; Um et al., 2013), and amylin receptors (Kimura et al., 2012).

However, A $\beta$  is not only extracellular but also accumulates intracellularly where it may interact with additional targets relevant for LTP inhibition, synapse loss, and cognitive impairment. Furthermore, exogenously-added A $\beta$  can enter cells from the medium. Indeed, we recently found that A $\beta$ (1-42) inhibits the activity of the microtubule-dependent motor protein Eg5/Kinesin-5 (also known as KIF11), which regulates a number of different important microtubule-dependent functions in neuronal and non-neuronal cells, including chromosome segregation, growth cone turning, and microtubule organization in axons and dendrites that may also indirectly impact membrane trafficking (Ari et al., 2014; Baas et al., 1998; Borysov et al., 2011; Ferhat et al., 1998; Kahn et al., 2015; Nadar et al., 2008). LTP is induced by Ca<sup>2+</sup> influx through NMDARs and is expressed by increased function of  $\alpha$ -amino-3-hydroxy-5-methyl-4-isoxazolepropionic acid (AMPA) glutamate receptors (AMPA receptors) that are recruited to the synapse via membrane trafficking. Alterations in membrane trafficking of NMDARs and AMPARs as well as phosphorylation of microtubule regulatory proteins such as tau are thought to be particularly relevant for A $\beta$ -mediated synaptic dysfunction (reviewed in Mucke and Selkoe, 2012). Thus, here we further investigated possible roles for Eg5 inhibition in A $\beta$ (1-42)-mediated synaptic dysfunction, by exploring the similarity of actions of monastrol, a specific small molecule inhibitor of Eg5 (Cochran et al., 2005; Maliga et al., 2002), with those of A $\beta$ (1-42) on acute inhibition of LTP in hippocampal slices and on chronic promotion of dendritic spine/synapse loss in neuronal cultures. Importantly, our findings are consistent with A $\beta$  promoting synaptic dysfunction at least in part through inhibition of Eg5/Kinesin-5.

## Materials and Methods

### *Animals*

Experiments were performed on C57/BL6 male mice, 14-21 days old. All animal procedures were conducted in accordance with NIH-PHS guidelines and with the approval of the University of Colorado, Denver Institutional Animal Care and Use Committee.

### *Pharmacologic Reagents*

All chemical were obtained form Sigma, except where noted otherwise. CNQX and APV were obtained from Tocris. Monastrol was obtained from Sigma. Synthetic A $\beta$ (1-42) peptide was obtained from Anaspec and stock solutions were prepared as follows: Method 1) For electrophysiology experiments, 1 mg A $\beta$ (1-42) was dissolved in 80  $\mu$ l NH<sub>4</sub>OH (1 M) + 120  $\mu$ l DMSO (final concentration 1.1 mM), aliquoted, flash frozen, and stored at -80°C until use. Aliquots were then thawed on the day of use and diluted to the appropriate working concentration(s) in aCSF; Method 2) For dendritic spine loss experiments, 1 mg A $\beta$ (1-42) was dissolved in 440  $\mu$ l 1,1,1,3,3,3-hexafluoro-2-propanol, aliquoted per 100  $\mu$ g, the 1,1,1,3,3,3-hexafluoro-2-propanol evaporated under nitrogen, and then the dried A $\beta$ (1-42) peptide stored at -80°C until use. On the day before use, a single A $\beta$ (1-42) peptide aliquot was dissolved in 2.2  $\mu$ l DMSO for 1 hr at room temperature, diluted with PBS to a concentration of 100  $\mu$ M, stored for 24 hrs at 4°C, centrifuged at 14,000xg for 10 min, and the supernatant removed. This supernatant was then diluted into the neuronal culture media to achieve the desired final working concentration(s). Using either of these methods, the resulting solutions contained predominantly A $\beta$ (1-42) monomers and low-molecular weight soluble oligomers (dimers and trimers), with no detectable presence of higher molecular weight species as shown in Figure 1 by electrophoresis under non-denaturing conditions on 10-20% Tris-Tricine gels (BioRad), transfer to 0.2  $\mu$ m reinforced nitrocellulose (Whatman), and immunoblotting with anti-A $\beta$  antibodies (Covance; 1:10,000).

## ***Electrophysiology***

*Mouse Hippocampal Slice Preparation.* After sacrifice, the brains were rapidly removed and immersed in ice-cold, sucrose containing cutting buffer (in mM: 2 KCl, 12 MgCl<sub>2</sub>, 0.2 CaCl<sub>2</sub>, 1.25 NaH<sub>2</sub>PO<sub>4</sub>, 10 D-glucose, 220 sucrose, and 26 NaHCO<sub>3</sub>) for 40-60 s to cool the interior of the brain. Transverse slices (400 μm thickness) were made using a McIlwain tissue chopper/slicer, and then slices were transferred to individual compartments in a storage system for at least 60 min. After recovery, a single slice was transferred to a recording chamber and superfused with artificial cerebrospinal fluid (aCSF) at a bulk flow rate of 2-3 ml/min at 31°C. The aCSF contained the following (in mM): 124 NaCl, 3.5 KCl, 1.3 MgCl<sub>2</sub>, 2.5 CaCl<sub>2</sub>, 1.2 NaH<sub>2</sub>PO<sub>4</sub>, 11 D-glucose, 25.9 NaHCO<sub>3</sub> and 0.0025 picrotoxin (Tocris).

*Baseline Recordings.* Before each slice recording experiment, an input-output curve was generated by increasing the stimulus voltage and recording the synaptic response until either a maximum was reached, or evidence of a population spike was observed on the field excitatory postsynaptic potential (fEPSP) response.

*LTP Measurements.* Synaptic fEPSP responses were evoked with bipolar tungsten electrodes placed in Schaffer collateral axon pathway to the CA1 dendritic field layer. Test stimuli were delivered once every 20 seconds with the stimulus intensity set to 40-50% of the maximum synaptic response. HFS consisted of two trains of 100 Hz stimuli lasting 1 second each, with an inter-train interval of 20 seconds, at the control stimulus intensity. fEPSP recordings were made with a glass micropipette filled with aCSF and placed in the stratum radiatum approximately 200-300 μm from the cell body layer. This stimulation produced LTP that persisted for more than 60 min in WT animals. The initial slopes of fEPSPs were calculated as the slope measured between 10-30% from the origin of the initial negative deflection. Each time point shown is an average of six 20 sec interval measurements. An average over 10 min of LTP recordings 55-65 minutes after HFS were used in the summary analyses.

### **Neuronal cultures**

Hippocampal neuron cultures were prepared from postnatal day 0-2 C57/BL6 male and female mice, plated at medium density (300-450 cells/mm<sup>2</sup>) on glass coverslips and maintained in Neurobasal plus B27 (Invitrogen) and GlutaMAX (Invitrogen) until transfection with a plasmid encoding green fluorescent protein (GFP)(pEGFPN1; Clontech) using Lipofectamine 2000 (Invitrogen) on *day-in-vitro* (DIV) 11-12 as previously described (Robertson et al, 2009; Keith et al., 2012). After 1 day of GFP expression on DIV 12-13, the cultures were then left untreated (controls) or treated for two additional days with A $\beta$ (1-42) and/or monastrol added to the culture media. On DIV 14-15 after treatment, neurons were fixed in 3.7% formaldehyde and then the coverslips mounted on slides with Pro-Long Gold (Invitrogen). Images of GFP transfected dendrites were then acquired on an Axiovert 200M microscope (Zeiss) with a 63x objective (1.4NA, plan-Apo) and a CoolSNAP2 (Photometrics) CCD camera. Focal plane z-stacks (0.5  $\mu$ m spacing) were acquired, deconvolved to correct for out of focus light, and 2D maximum intensity projections generated (Slidebook 5.0-6.0, Intelligent Imaging Innovations). Spine numbers were quantified from projection images using the ruler tool in Slidebook 5.0-6.0 software with manual counting as in Robertson et al, 2009 and expressed as the number of spines / 10  $\mu$ m of dendrite using measurements obtained for multiple lengths of dendrite (N = number of lengths of dendrite) taken from multiple images across three independent neuronal cultures for each experimental treatment condition.

### **Statistical Methods**

Group comparisons to control were performed in Prism (GraphPad) using one-way ANOVA followed by Dunnet's post hoc analysis, in which case only  $p > 0.05$  (not significant), \* $p < 0.05$ , \*\* $p < 0.01$  and \*\*\* $p < 0.001$  are provided by the software. Pair-wise comparisons were performed in Prism or Excel (Microsoft) using Student's t-test. In all cases significance is reported as  $p < 0.05$  and data are expressed as mean  $\pm$  SEM error bars.

## Results

Many previous studies have shown that acute application of A $\beta$ (1-42) can inhibit LTP at hippocampal CA1 synapses. Accordingly, we confirmed that 20 min pre-incubation of hippocampal slices with 100 nM A $\beta$ (1-42) strongly inhibited LTP of the AMPAR synaptic response measured as the slope of the field excitatory postsynaptic potential (fEPSP) by extracellular recording at CA1 synapses (Figure 2A, B). We further investigated whether disabling one of the intracellular, cytosolic targets of A $\beta$ (1-42), the microtubule-dependent motor protein Eg5/Kinesin-5, might also block LTP. Importantly, 20 min pre-incubation with 100 nM monastrol, a specific Eg5 inhibitor, also strongly inhibited LTP (Figure 2A,B). Additional dose-response analyses demonstrated that a wide range of concentrations of A $\beta$ (1-42) from 20 nM to 1  $\mu$ M and monastrol from 100 nM to 100  $\mu$ M caused essentially complete inhibition of LTP. However, slightly lower concentrations of 1 nM A $\beta$ (1-42) and 50 nM monastrol only partially inhibited LTP, with each causing a non-significant trend toward approximately 50% suppression (Figure 2C).

Next we attempted to learn whether A $\beta$ (1-42) may act through the same mechanism(s) as monastrol, that is, by inhibiting Eg5. Thus, we applied each compound together at the concentrations that produced non-significant, partial LTP inhibition when tested alone, to determine whether there would be any additional inhibition when co-applied. Importantly, when 1 nM A $\beta$ (1-42) and 50 nM monastrol were applied together LTP was completely inhibited (Figure 3A,B). This enhanced inhibition suggests that A $\beta$ (1-42) and monastrol may each partially inhibit the same mechanism(s) required for LTP, such that when added together more complete inhibition of LTP results. However, from these pharmacologic results alone, we cannot rule out that these two agents may also inhibit LTP in part through separate mechanisms.

A $\beta$ (1-42) and/or monastrol could inhibit LTP through altering NMDAR activity that is necessary for LTP induction or by eventually suppressing AMPAR activity that is required for maintenance of LTP

expression. We investigated the first possibility by studying NMDAR component of the fEPSP pharmacologically isolated by using 10  $\mu$ M CNQX to block AMPARs and increasing the stimulus intensity. A test concentration of 100 nM A $\beta$ (1-42), which is higher than required to completely inhibit LTP (Figure 2C), when applied for 60 min did not alter either the slope or amplitude of these isolated NMDAR synaptic responses (Figure 4A). In contrast, application of 200 nM monastrol, which is also higher than that required to completely inhibit LTP (Figure 2C), did cause a gradual and slight, but persistent, reduction ( $\sim$  20-25%) in NMDAR responses, but this reduction only became significant after 60 min of treatment ( $***p < 0.001$ ; at end of drug application and persisting after washout)(Figure 4B). Importantly, no significant inhibition of NMDAR activity was observed after only 20 min of treatment with monastrol (i.e., at the time when HFS was delivered to induce LTP in Figures 2 and 3). Thus, NMDAR inhibition was not responsible for acute LTP inhibition by either A $\beta$ (1-42) or monastrol in our experiments above. Likewise, neither 100 nM A $\beta$ (1-42) (Figure 4C) nor 200 nM monastrol (Figure 4D) resulted in any inhibition of the slope or amplitude of AMPAR fEPSP responses over 60 min of application and following washout for 30 min. Thus, direct inhibition of AMPAR transmission cannot account for the inhibitory actions of A $\beta$ (1-42) or monastrol on LTP.

While we did not observe any decreases in synaptic AMPAR or NMDAR responses with only 1 hour exposure to A $\beta$ (1-42), previous studies have found that more prolonged exposure to higher amounts of A $\beta$ (1-42) can substantially reduce synaptic NMDAR and AMPAR currents and also trigger synapse loss over a period of several days (Hsieh et al., 2006; Shankar et al., 2007). In addition, prolonged exposure to A $\beta$ (1-42) or monastrol can also lead to reduced surface expression of AMPAR and NMDAR subunits (Ari et al, 2014; Snyder et al., 2006), perhaps due to both enhanced endocytosis and impaired delivery to the plasma membrane. Given that we observed a small reduction in synaptic NMDAR activity after 1 hour of Eg5 inhibition with a monastrol, we next examined the impacts of longer A $\beta$ (1-42) and monastrol treatments on the number of dendritic spines in cultured mouse hippocampal

neurons as an indicator of synapse loss (Figure 5). In agreement with many previous studies showing A $\beta$ (1-42)-induced synapse loss, application of 0.25-1  $\mu$ M A $\beta$ (1-42) for 48 hours caused a concentration-dependent reduction in the number of spines (up to  $\sim$  35% maximum loss; Figure 5A,B). Similarly, monastrol (0.5-5  $\mu$ M) treatment also resulted in comparable spine loss ( $\sim$  40% maximum loss). We then examined the effect of adding both A $\beta$ (1-42) and monastrol together on spine loss. Treatment with 0.5  $\mu$ M A $\beta$ (1-42) in addition to 5  $\mu$ M monastrol also resulted in  $\sim$ 40% loss of spines (Figure 4), which was approximately the same degree of spine loss observed for each compound alone. Thus, the spine loss promoted by monastrol occluded any additional spine loss by A $\beta$ (1-42), a result that is consistent with shared/overlapping mechanisms for reduction in spine density by A $\beta$ (1-42) and monastrol in hippocampal neurons.

## Discussion

AD is a neurodegenerative disorder that disrupts memory and cognitive abilities. The underlying molecular mechanisms of AD are diverse, but one of the primary lines of current research is that soluble oligomeric forms of A $\beta$ (1-42) and A $\beta$ (1-40) accumulate in and around excitatory synapses to alter normal processes of learning long before the appearance of amyloid plaques and neuronal cell loss. In particular, many studies have shown that A $\beta$ (1-42) blocks LTP (Chen et al., 2000; Selkoe, 2008; Walsh et al., 2002), a cellular mechanism thought to underlie memory acquisition. Data presented here confirms that a range of A $\beta$ (1-42) concentrations applied to hippocampal slices *in vitro* inhibit LTP at Schaffer collateral to CA1 synapses.

A number of mechanisms have been proposed to explain how A $\beta$ (1-42) might block LTP, including endocytosis of synaptic NMDARs (Goto et al., 2006; Kurup et al., 2010; Snyder et al., 2006) and glutamate spillover resulting in overactivation of extrasynaptic NMDARs (O'Shea et al., 2008; Li et al., 2009), and in particular GluN2B-containing NMDARs (de Felice et al., 2007; Ferreira et al., 2010; Li et al., 2011; Mota et al., 2014; Shankar et al., 2007). Previous data from our lab indicate that both A $\beta$ (1-42) and monastrol result in reduced surface levels of NMDAR GluN1 and GluN2B subunits in cultured cells over several days, as measured by flow cytometry and confocal imaging (Ari et al., 2014). However, our data here are not consistent with any acute effect of A $\beta$ (1-42) or monastrol on synaptic NMDARs being responsible for LTP inhibition, as 20 min pre-incubation with A $\beta$ (1-42) or monastrol was sufficient to inhibit LTP but had no significant impact on pharmacologically isolated NMDA fEPSPs. Indeed, A $\beta$ (1-42) showed no inhibition and monastrol only caused partial (~20-25%) inhibition of NMDAR responses even after 60 min. However, previous work by Raymond et al. (2003) did observe ~ 25% inhibition of NMDAR fEPSPs with only 20 min application of 200 nM A $\beta$ (1-40). Yet, even in that study partial inhibition of NMDARs could not account for the complete inhibition of LTP by A $\beta$ , because direct antagonism of NMDARs producing comparable inhibition of NMDAR fEPSPs did not alter LTP (Raymond et al., 2003). In

addition, both our findings here and those of Raymond et al. are consistent with another previous study that observed acute A $\beta$ (1-42) inhibition of LTP without any significant inhibition of synaptic NMDAR currents in whole-cell recordings of CA1 neurons (Nomura et al., 2005). Thus, longer applications of A $\beta$ (1-42) than 60 min are likely necessary to observe substantial reductions in synaptic NMDAR responses as documented in other previous studies (Hsieh et al., 2006; Shankar et al, 2007).

Another process important for both synapse maintenance and LTP expression is the trafficking of AMPARs and other synaptic proteins to and from the synapse (Huganir and Nicoll, 2013). Our previous work indicated that A $\beta$ (1-42) increased chromosome mis-segregation and aneuploidy (Granic et al., 2010) in cells due to A $\beta$ (1-42) interfering with correct mitotic spindle formation through inhibiting the Eg5 microtubule motor (Borysov et al., 2011). Importantly, Eg5 is also involved in regulating the organization and stability of microtubules in axons and dendrites, and thus may also indirectly impact microtubule-dependent receptor trafficking (Ari et al., 2014; Kahn et al., 2015; Nadar et al., 2008). We previously found that a high concentration of monastrol (100  $\mu$ M) inhibited LTP (Ari et al., 2014). We confirmed that result here and further found that much lower concentrations of monastrol from 100 nM-1  $\mu$ M also inhibit LTP to levels that are comparable to those observed with as little as 20-100 nM A $\beta$ (1-42). Importantly, 50 nM A $\beta$ (1-42) was previously shown to directly inhibit the activity of Eg5 and two other related motor proteins, KIF4A and MCAK (Borysov et al., 2011). However, interestingly we observed LTP inhibition with as little as 100 nM monastrol, which is below the low  $\mu$ M IC<sub>50</sub> values previously measured for direct inhibition of Eg5 motor domain activity *in vitro* (Cochran et al., 2005). However, LTP is a very complex, non-linear phenomenon and we do not yet know how Eg5 function is integrated into its underlying mechanisms; thus it is difficult to predict the sensitivity of LTP to inhibition by monastrol, or even A $\beta$ , based solely on extrapolation from *in vitro* biochemical studies with isolated protein domains. For instance, it is possible that monastrol inhibition of LTP could involve not only direct inhibition of Eg5 motor activity but also downstream changes in the functions of other microtubule

regulatory proteins, such as tau, which is known to mediate some, but not all, of the impacts of A $\beta$  on neuronal functions (reviewed in Mucke and Selkoe, 2012), including membrane trafficking (Umeda et al., 2015; Vossel et al., 2015). Accordingly, a recent study found that tau can also inhibit Eg5 activity, thus A $\beta$  may inhibit Eg5 not only directly but also indirectly via regulation of tau (Bouge and Parmentier, 2016). Overall, it is likely that there is very complex interplay between A $\beta$ , tau, and Eg5 in regulation of neuronal function that definitely warrants future investigation.

Regulation of AMPAR trafficking, in particular, has received considerable attention in the mechanisms of A $\beta$ -induced neuronal dysfunction, because A $\beta$ (1-42) can promote AMPAR endocytosis to favor synaptic depression (Hsieh et al, 2006). Indeed, application of A $\beta$ (1-42) has been observed to result in reductions of surface AMPARs and AMPAR synaptic currents, and reduced levels of surface AMPARs have also been observed in AD transgenic mice (Almeida et al., 2005; Hsieh et al, 2006; Roselli et al., 2005; Snyder et al., 2006; Zhao et al., 2010). Yet, in our LTP experiments we found no decrease in AMPAR basal transmission during ~20 min A $\beta$  or monastrol pre-incubation before LTP induction. In addition, even when applied for 60 min neither A $\beta$  nor monastrol caused a decrease in AMPAR fEPSPs. Thus, direct promotion of AMPAR synaptic depression did not contribute to the LTP inhibition we observed for A $\beta$  or monastrol. However, the substantial dendritic spine loss we observed with chronic A $\beta$  or monastrol treatment is likely to be associated with glutamate receptor endocytosis and suppression of both AMPAR and NMDAR-mediated synaptic transmission, as seen in previous studies examining spine loss and synaptic dysfunction in neuronal cultures chronically exposed to A $\beta$ (1-42) (Hsieh et al., 2006; Shankar et al., 2007).

Because we found that low-moderate concentrations of either A $\beta$ (1-42) or monastrol were sufficient to completely inhibit LTP on their own, we were unable to clearly test whether LTP inhibition by co-treatment with A $\beta$  oligomers and monastrol shows reciprocal occlusion (i.e., acting exclusively

through the same mechanism(s)). However, lower doses of A $\beta$ (1-42) (1 nM) and monastrol (50 nM), which at best partially inhibited LTP on their own, resulted in much more pronounced LTP inhibition when administered together. In other words, monastrol-mediated inhibition of Eg5 appeared to sensitize CA1 synapses to the inhibitory effect of A $\beta$ (1-42) on LTP. Importantly, while monastrol and A $\beta$  both inhibit Eg5 ATPase-dependent motor activity through mechanisms that are competitive with respect to regulation by microtubules, monastrol slows release of ADP and A $\beta$  competes with ATP binding (Borysov et al., 2011; Cochran et al., 2005). Thus, additive inhibition could be expected for low concentrations of monastrol and A $\beta$  even if both are converging on Eg5. In addition, A $\beta$  (but not monastrol) inhibits the related motor proteins KIF4A and MCAK, which are both also expressed in neurons and could share functions with Eg5 that are required for LTP (Borysov et al., 2011).

Regardless of these remaining uncertainties for acute LTP inhibition, our comparison of the impacts of chronic co-treatment with A $\beta$ (1-42) and monastrol on dendritic spine loss in cultured hippocampal neurons provided even clearer evidence that A $\beta$  and monastrol share common downstream molecular mechanisms. In particular, we observed no additional spine loss following co-treatment with higher doses of monastrol (5  $\mu$ M) and A $\beta$ (1-42) (0.5  $\mu$ M) that each alone triggered a maximum of 35-40% spine loss. Thus, overall, we found that monastrol can mimic, and in some cases occlude, the impacts of A $\beta$ (1-42) on excitatory synapses, suggesting that A $\beta$ (1-42) may induce both acute and chronic synaptic dysfunction in part through inhibiting Eg5.

Dendritic spine loss is observed in both cortical and hippocampal regions in humans with AD. In addition, spine loss and hippocampal LTP impairments are seen even at the very earliest stages of AD in mouse models when learning and memory alterations are also first evident, but before amyloid plaque and neurofibrillary tangles are observed (reviewed in Mucke and Selkoe, 2012). Our findings that the microtubule-dependent motor Eg5 is inhibited by A $\beta$  oligomers and that direct Eg5 inhibition by

monastrol can closely phenocopy both acute A $\beta$  LTP inhibition and chronic A $\beta$ -induced spine loss suggest that A $\beta$  may disrupt microtubule-dependent neuronal functions, not only through its known regulation of tau, but also through its inhibition of Eg5. In particular, inhibiting Eg5 may have a variety of impacts on the dendritic cytoskeleton that directly or indirectly alter spine structure, synaptic function, and LTP during even the earliest stages of AD. These results also suggest that blocking A $\beta$  inhibition of Eg5/Kinesin-5 could provide a novel approach for developing AD therapies.

**Authorship Contributions:**

*Participated in research design:* Potter, Freund, Dell'Acqua

*Conducted experiments:* Gibson, Freund

*Performed data analysis:* Freund, Dell'Acqua, Gibson

*Wrote or contributed to the writing of the manuscript:* Freund, Potter and Dell'Acqua

## References

- Almeida CG, Tampellini D, Takahashi RH, Greengard P, Lin MT, Snyder EM, and Gouras GK (2005)  $\beta$ -amyloid accumulation in APP mutant neurons reduces PSD-95 and GluR1 in synapses. *Neurobiol Dis* **20**:187–198
- Ari C, Borysov SI, Wu J, Padmanabhan J, and Potter H (2014) Alzheimer amyloid beta inhibition of Eg5/kinesin 5 reduces neurotrophin and/or transmitter receptor function. *Neurobiol Aging* **35**:1839-49.
- Baas PW (1998) The role of motor proteins in establishing the microtubule arrays of axons and dendrites. *J Chem Neuroanatomy* **14**:175-80.
- Borysov SI, Granic A, Padmanabhan J, Walczak, CE and Potter H (2011) Alzheimer A $\beta$  disrupts the mitotic spindle and directly inhibits mitotic microtubule motors. *Cell Cycle* **10**:1397-1410.
- Bourge AL and Parmentier ML (2016) Tau excess impairs mitosis and kinesin-5 function, leading to aneuploidy and cell death. *Dis Model Mech* doi: 10.1242/dmm.022558 [Epub ahead of print].
- Chen Q-S, Kagan BL, Hirakura Y, and Xie C-W (2000) Impairment of hippocampal long-term potentiation by Alzheimer amyloid  $\beta$ -peptides. *J Neurosci Res* **60**:65-72.
- Cochran JC, Gatial III JE, Kapoor TM, and Gilbert SP (2005) Monastrol inhibition of the mitotic kinesin Eg5. *J Biol Chem* **280**:12658-12667.
- Dickson DW, Crystal HA, Bevona C, Honer W, Vincent I, and Davies P (1995) Correlations of synaptic and pathological markers with cognition of the elderly. *Neurobiol Aging* **16**:285–298.
- De Felice FG, Velasco PT, Lambert MP, Viola K, Fernandez SJ, Ferreira ST, and Klein WL (2007) A $\beta$  oligomers induce neuronal oxidative stress through an N-methyl-d-aspartate receptor-dependent mechanism that is blocked by the Alzheimer drug memantine. *J Biol Chem* **282**:11590–11601.

Ferhat L, Cook C, Chauviere M, Harper M, Kress M, Lyons GE, and Baas PW (1998) Expression of the mitotic motor protein Eg5 in postmitotic neurons: implications for neuronal development. *J Neurosci* **18**:7822-35.

Ferreira IL, Bajouco LM, Mota SI, Auberson YP, Oliveira CR, and Rego, AC (2012) Amyloid beta peptide 1-42 disturbs intracellular calcium homeostasis through activation of GluN2B-containing N-methyl-d-aspartate receptors in cortical cultures. *Cell Calcium* **51**:95-106.

Goto Y, Niidome T, Akaike A, Kihara T, and Sugimoto H (2006) Amyloid beta-peptide preconditioning reduces glutamate-induced neurotoxicity by promoting endocytosis of NMDA receptor. *Biochem Biophys Res Commun* **351**:259–265.

Granic A, Padmanabhan J, Norden M, and Potter H (2010) Alzheimer A $\beta$  peptide induces chromosome mis-segregation and aneuploidy, including trisomy 21: requirement for Tau and APP. *Mol Biol Cell* **21**:511-520.

Hsieh H, Boehm J, Sato C, Iwatsubo T, Tomita T, Sisodia S, and Malinow R (2006) AMPAR removal underlies Abeta-induced synaptic depression and dendritic spine loss. *Neuron* **52**:831-843.

Huganir RL and Nicoll RA (2013) AMPARs and Synaptic Plasticity: The Last 25 Years. *Neuron* **80**:707-714.

Kahn OI, Sharma V, Gonzalez-Billault C, and Baas PW (2015) Effects of kinesin-5 inhibition on dendritic architecture and microtubule organization. *Mol Biol Cell* **26**:66-77.

Keith DJ, Sanderson JL, Gibson ES, Woolfrey KM, Robertson HR, Olszewski K, Kang R, El-Husseini A, and Dell'Acqua ML (2012) Palmitoylation of A-Kinase anchoring protein 79/150 regulates dendritic endosomal targeting and synaptic plasticity mechanisms. *J Neurosci* **32**:7119-7136.

Kim T, Vidal GS, Djuricic M, William CM, Birnbaum ME, Garcia KC, Hyman BT, and Shatz CJ (2013) Human LILRB2 is a  $\beta$ -amyloid receptor and its murine homolog PirB regulates synaptic plasticity in an Alzheimer's model. *Science* **341**:1399-404.

Kimura R, MacTavish D, Yang J, Westaway D, and Jhamandas JH (2012) Beta amyloid-Induced depression of hippocampal long-term potentiation is mediated through the amylin receptor. *J Neurosci* **32**:17401–17406.

Kurup P, Zhang Y, Xu J, Venkitaramani DV, Haroutunian V, Greengard P, Nairn AC and Lombroso PJ (2010) A $\beta$ -mediated NMDA receptor endocytosis in Alzheimer's disease involves ubiquitination of the tyrosine phosphatase STEP61. *J Neurosci* **30**: 5948–5957.

Lambert MP, Barlow AK, Chromy BA, Edwards C, Freed R, Liosatos M, Morgan TE, Rozovsky I, Trommer B, Viola KL, Wals P, Zhang C, Finch CE, Krafft GA, and Klein WL (1998) Diffusible, nonfibrillar ligands derived from A $\beta$ 1–42 are potent central nervous system neurotoxins. *Proc Natl Acad Sci USA* **95**: 6448–6453.

Laurén J, Gimbel DA, Nygaard HB, Gilbert JW, and Strittmatter SM (2009) Cellular prion protein mediates impairment of synaptic plasticity by amyloid-beta oligomers. *Nature* **457**:1128-32.

Li S, Hong S, Shepardson NE, Walsh DM, Shankar GM, and Selkoe D (2009) Soluble oligomers of amyloid beta protein facilitate hippocampal long-term depression by disrupting neuronal glutamate uptake. *Neuron* **62**:788–801.

Li S, Jin M, Koeglsperger T, Shepardson NE, Shankar GM, and Selkoe DJ (2011) Soluble A $\beta$  oligomers inhibit long-term potentiation through a mechanism involving excessive activation of extrasynaptic NR2B-containing NMDA receptors. *J Neurosci* **31**:6627–6638.

Liu Q, Huang Y, Shen J, Steffensen S and Wu J. (2012) Functional  $\alpha 7\beta 2$  nicotinic acetylcholine receptors expressed in hippocampal interneurons exhibit high sensitivity to pathological level of amyloid  $\beta$  peptides. *BMC Neuroscience* **13**:155.

McLean CA, Cherny RA, Fraser FW, Fuller SJ, Smith MJ, Beyreuther K, Bush AI, and Masters CL (1999) Soluble pool of A $\beta$  amyloid as a determinant of severity of neurodegeneration in Alzheimer's disease. *Ann Neurol* **46**:860–866.

Maliga Z, Kapoor TM, and Mitchison TJ (2002) Evidence that monastrol is an allosteric inhibitor of the mitotic kinesin Eg5. *Chem & Biol* **9**:989-996.

Mota SI, Ferreira IL, and Rego AC (2014) Dysfunctional synapse in Alzheimer's disease – A focus on NMDA receptors. *Neuropharmacology* **76**:16-26.

Mucke L and Selkoe DJ (2012) Neurotoxicity of amyloid beta-protein: synaptic and network dysfunction. *Cold Spring Harbor Perspectives in Medicine* **2**:a006338.

Naslund J, Haroutunian V, Mohs R, Davis KL, Davies P, Greengard P, and Buxbaum JD (2000) Correlation between elevated levels of amyloid  $\beta$ -peptide in the brain and cognitive decline. *JAMA* **283**:1571–1577.

Nadar VC, Ketschek A, Myers KA, Gallo G, Baas PW (2008) Kinesin-5 is essential for growth-cone turning. *Curr Biol* **18**:1972-1977.

O'Shea SD, Smith IM, McCabe OM, Cronin MM, Walsh DM, and O'Connor WT (2008) Intracerebroventricular administration of amyloid  $\beta$ -protein oligomers selectively increases dorsal hippocampal dialysate glutamate levels in the awake rat. *Sensors* **8**:7428–7437.

Nomura I, Kato, N, and Takechi H. (2005) Mechanism of impairment of long-term potentiation by amyloid  $\beta$  is independent of NMDA receptors or voltage-dependent calcium channels in hippocampal CA1 pyramidal neurons. *Neurosci Lett* **391**:1-6.

Raymond CR, Ireland DR, and Abraham WC (2003) NMDA Receptor regulation by amyloid- $\beta$  does not account for its inhibition of LTP in rat hippocampus. *Brain Res* **968**:263-272.

Robertson HR, Gibson ES, Benke TA, and Dell'Acqua ML (2009) Regulation of postsynaptic structure and function by an A-kinase anchoring protein-membrane associated guanylate kinase scaffolding complex. *J Neurosci* **29**:7929-7943.

Roselli F, Tirard M, Lu J, Hutzler P, Lamberti P, Livrea P, Morabito M, and Almeida OFX (2005) Soluble  $\beta$ -amyloid 1-40 induces NMDA-dependent degradation of postsynaptic density-95 at glutamatergic synapses. *J Neurosci* **25**:11061–11070.

Selkoe, DJ. (2008) Soluble oligomers of the amyloid  $\beta$ -protein impair synaptic plasticity and behavior. *Behav Brain Res* **192**:106–113.

Shankar GM, Bloodgood BL, Townsend M, Walsh DM, Selkoe DJ, and Sabatini BL (2007) Natural oligomers of the Alzheimer amyloid-beta protein induce reversible synapse loss by modulating an NMDA-type glutamate receptor-dependent signaling pathway. *J Neurosci* **27**:2866-2875.

Shankar G, Li S, Mehta T, Garcia-Munoz A, Shepardson N, Smith I, Brett F, Farrell M, Rowan M, Lemere C, Regan C, Walsh D, Sabatini B, and Selkoe D (2008) Amyloid- $\beta$  protein dimers isolated directly from Alzheimer's brains impair synaptic plasticity and memory. *Nat Med* **14**:837–842.

Snyder EM, Nong Y, Almeida CG, Paul S, Moran T, Choi EY, Nairn AC, Salter MW, Lombroso PJ, Gouras GK, and Greengard P (2005) Regulation of NMDA receptor trafficking by amyloid-beta. *Nat Neurosci* **8**:1051-1058.

Terry RD, Masliah E, Salmon DP, Butters N, DeTeresa R, Hill R, Hansen LA, and Katzman R (1991) Physical basis of cognitive alterations in Alzheimer's disease: synapse loss is the major correlate of cognitive impairment. *Ann Neurol* **30**:572–580.

Um JW, Kaufman AC, Kostylev M, Heiss JK, Stagi M, Takahashi H, Kerrisk ME, Vortmeyer A, Wisniewski T, Koleske AJ, Gunther EC, Nygaard HB, and Strittmatter SM (2013) Metabotropic glutamate receptor 5 is a coreceptor for Alzheimer A $\beta$  oligomer bound to cellular prion protein. *Neuron* **79**:887-902.

Umeda T, Ramser EM, Yamashita M, Nakajima K, Mori H, Silverman MA, and Tomiyama T (2015) Intracellular amyloid  $\beta$  oligomers impair organelle transport and induce dendritic spine loss in primary neurons. *Acta Neuropathologica Comm* **3**:51 DOI 10.1186/s40478-015-0230-2.

Vossel KA, Xu JC, Fomenko V, Miyamoto T, Suberbielle E, Knox JA, Ho K, Kim DH, Yu G-Q, and Mucke L (2015) Tau reduction prevents A $\beta$ -induced axonal transport deficits by blocking activation of GSK3 $\beta$ . *J Cell Biol* **209**:419-433.

Walsh DM, Klyubin I, Fadeeva JV, Cullen WK, Anwyl R, Wolfe MS, Rowan MJ, and Selkoe DJ (2002) Naturally secreted oligomers of amyloid  $\beta$  protein potently inhibit hippocampal long-term potentiation in vivo. *Nature* **416**:535-539.

Wang HY, Lee DH, D'Andrea MR, Peterson PA, Shank RP, and Reitz AB (2000a) Beta-amyloid (1–42) binds to alpha7 nicotinic acetylcholine receptor with high affinity. Implications for Alzheimer's disease pathology. *J Biol Chem* **275**:5626–5632.

Wang HY, Lee DH, Davis CB, and Shank RP (2000b) Amyloid peptide A $\beta$ (1–42) binds selectively and with picomolar affinity to alpha7 nicotinic acetylcholine receptors. *J Neurochem* **75**:1155–1161.

Wimo A and Prince M (2011) World Alzheimer Report 2010: The Global Economic Impact of Dementia. Alzheimer's Disease International [online], <http://www.alz.co.uk/research/files/WorldAlzheimerReport2010.pdf>.

Zhao W-Q, Santini F, Breese R, Ross D, Zhang XD, Stone DJ, Ferrer M, Townsend M, Wolfe AL, Seager MA, Kinney GG, Shughrue PJ, and Ray WJ (2010) Inhibition of calcineurin-mediated endocytosis and  $\alpha$ -

amino-3-hydroxy-5-methyl-4- isoxazolepropionic acid (AMPA) receptors prevents amyloid  $\beta$  oligomer-induced synaptic disruption. *J Biol Chem* **285**:7619–7632.

**Footnotes:**

\*This work was supported by grants from the National Institutes of Health National Institute of Neurological Disorders and Stroke to HP [Grant# NS076291] and to MLD [Grant# NS040701] and support from the Linda Crnic Institute for Down Syndrome to HP and MLD. Contents are the authors' sole responsibility and do not necessarily represent official NIH views. The authors declare no competing financial interests.

†Reprint requests can be addressed to Mark L. Dell'Acqua, Dept. of Pharmacology, 12800 E. 19<sup>th</sup> Ave, Mail Stop 8303, Aurora, CO 80045. Email: [mark.dellacqua@ucdenver.edu](mailto:mark.dellacqua@ucdenver.edu)

## Figure Legends

**Figure 1.** Preparation of soluble, low molecular weight A $\beta$ (1-42) oligomers. Non-denaturing 10-20% Tris-Tricine gel electrophoresis and immunoblotting with anti-A $\beta$  antibodies demonstrates successful preparation of solutions containing predominantly A $\beta$ (1-42) monomers and low-molecular weight, soluble oligomers (dimers and trimers), with no detectable presence of higher molecular weight species. Both preparation method 1, used for slice electrophysiology experiments, and method 2, used for neuronal culture spine loss experiments, produce similar results. Note: Under non-denaturing conditions it is difficult to make accurate MW determinations based on relative migration compared to MW standards.

**Figure 2.** Inhibition of early phase (up to one hour) of long-term potentiation (LTP) by A $\beta$ (1-42) and monastrol. **(A)** Typical field excitatory post-synaptic potentials (fEPSPs) before (black lines) and 60 min following (gray lines) high-frequency stimulation (HFS). **(B)** Time course of slope of fEPSPs before and after 2 HFS trains (black arrow: 1 x 100 Hz, 20 sec apart). Open bar indicates time of drug application. A $\beta$ (1-42) (100 nM) or monastrol (100 nM) were applied to the bath 20 min prior to, and including HFS, and the slopes and amplitudes of fEPSPs were recorded for 60 min following HFS. Numbers (1, 2) on time course indicate times when example signals in panel A were obtained. Data represent mean  $\pm$  SEM for 5 slices from 4 animals for A $\beta$ (1-42) and for monastrol. **(C)** % LTP as a percent of baseline slope (average of 50-60 min.) for control (open bar) and various concentrations of A $\beta$ (1-42) (blue bars) and monastrol (red bars). Data represent mean  $\pm$  SEM for 4-5 slices from 3-5 mice for each concentration. Significance from control LTP was determined by one-way ANOVA with Dunnett's post-hoc analysis.

\*p < 0.05, \*\*p < 0.01, \*\*\*p < 0.001.

**Figure 3.** Inhibition of LTP by lower concentrations of A $\beta$ (1-42), monastrol, and A $\beta$ (1-42) plus monastrol. **(A)** Time course for control (open black circles, n = 9; from same experiments as in Figure 2B), 1 nM A $\beta$ (1-42) (solid blue squares, n = 5; from same experiments as in Figure 2C), 50 nM monastrol (solid red triangles, n = 8; from same experiments as in Figure 2C) and 1 nM A $\beta$ (1-42) plus 50 nM monastrol (solid purple diamonds, n = 9). Drugs were applied 20 min prior to and during HFS (100 Hz, 1 sec, 2 trains 20 sec apart). Data are mean slopes  $\pm$  SEM. **(B)** Bar graphs depicting mean % potentiation  $\pm$  SEM over control during last 10 min of recording period. At these concentrations, neither A $\beta$ (1-42) nor monastrol alone resulted in significant reduction of LTP, but when added together there was a significant, complete inhibition of LTP (one-way ANOVA with Dunnett's post-hoc; \*\*\* p < 0.001).

**Figure 4.** Time course of A $\beta$ (1-42) and monastrol impacts on baseline NMDAR and AMPAR field potentials. **(A)** Upper panel depicts a representative fEPSP response before (light grey) and after (dotted black) pharmacological isolation of the NMDAR component by blocking the AMPAR component of the response with 10  $\mu$ M CNQX. Traces are normalized to the peak of the response to better show the distinct, slower kinetics of the isolated NMDAR component of the fEPSP. The isolated NMDAR fEPSP response is completely inhibited with 100  $\mu$ M of the antagonist DL-APV (grey). Lower panel: time course of amplitudes and slopes of isolated NMDAR fEPSPs during application of 100 nM A $\beta$ (1-42) (n = 8). **(B)** Upper panel: representative isolated NMDAR fEPSPs before (1, black) and ~60 min after (2, light grey) application of monastrol. Lower panel: time course of amplitudes and slopes of isolated NMDAR fEPSPs before, during and after application of 100 nM monastrol (n = 6). One-way ANOVA followed by Dunnett's post-hoc analysis depicts no significant change after 20 min application of monastrol, but significant decreases (\*\*\*p < 0.001) in amplitude and slope at 60 and 90 min (the latter after 30 min. wash). Calibration bars in upper panels: 1 mV, 20 ms. **(C)** Time course of amplitudes and slopes of

AMPA fEPSPs during application of 100 nM A $\beta$ (1-42) (n = 5). **(D)** Time course of amplitudes and slopes of AMPAR fEPSPs during application of 200 nM monastrol (n = 6).

**Figure 5.** Dendritic spine loss following incubation of cultured mouse hippocampal neurons with A $\beta$ (1-42), monastrol, or both. **(A)** Neurons were transfected at 11-12 div to express GFP for visualization of dendritic spines. Neurons were left untreated (Control) or treated with the indicated concentrations of A $\beta$ (1-42) or monastrol or both for 48 hrs prior to fixation at 14-15 div. GFP fluorescence in dendrites was imaged by acquiring 3D image z-stacks (500 nm spacing) that were deconvolved to the nearest-neighbor and then collapsed into 2D maximum intensity projection images. **(B)** Dendritic spine density was then quantified from projection images as the number of dendritic spines/10  $\mu$ m length of dendrite. **(C)** Maximal spine loss was obtained at 0.5  $\mu$ M A $\beta$ (1-42) and 5  $\mu$ M monastrol; when applied together, no additional spine loss was observed. In Figure 5C, data graphed for Control, 0.5  $\mu$ M A $\beta$ (1-42), and 5  $\mu$ M monastrol alone are same as in Figure 5B. N=17-34 lengths of dendrite analyzed per condition. Data are mean  $\pm$  SEM. \*p < 0.05, \*\*p < 0.01 to Control by ANOVA with Dunnett's post-hoc.

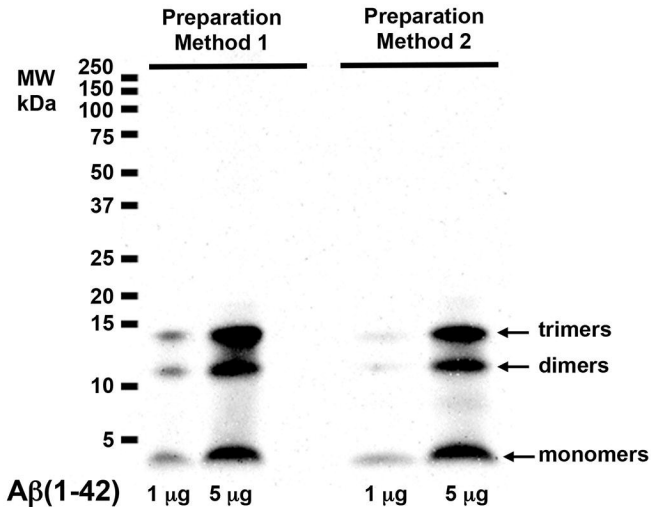
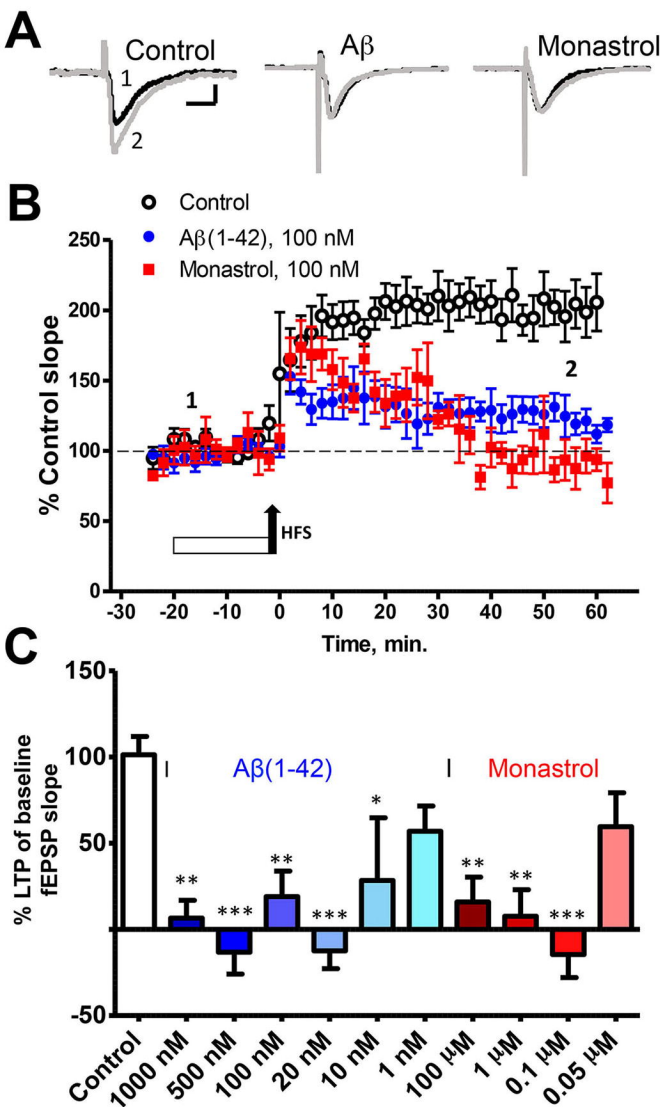
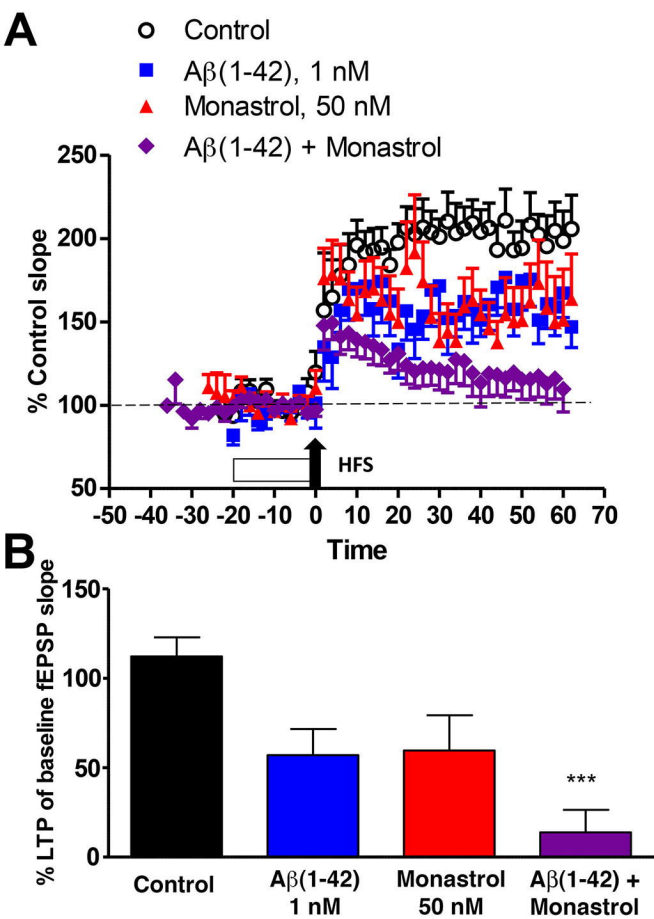


Figure 1



**Figure 2**



**Figure 3**

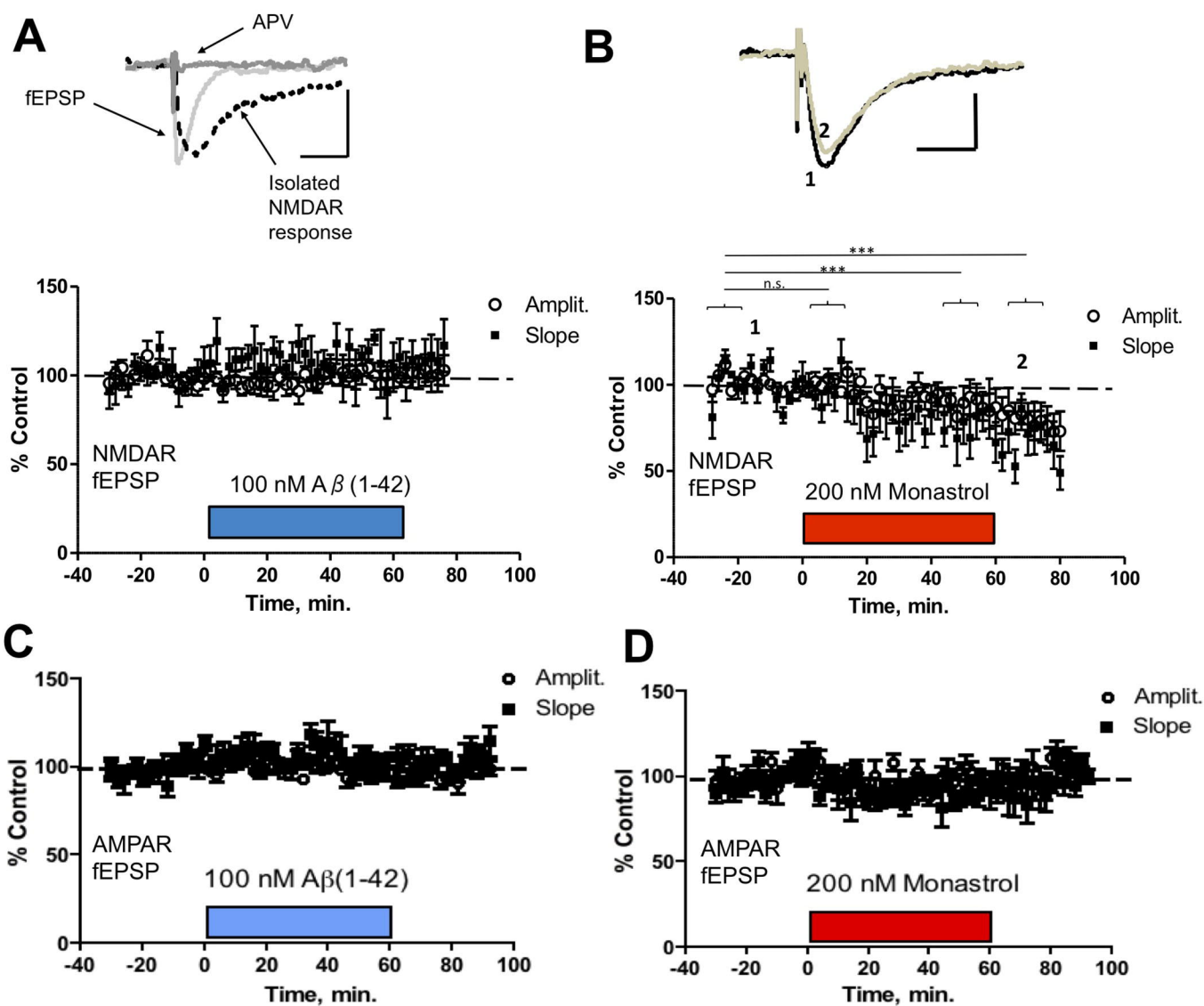


Figure 4

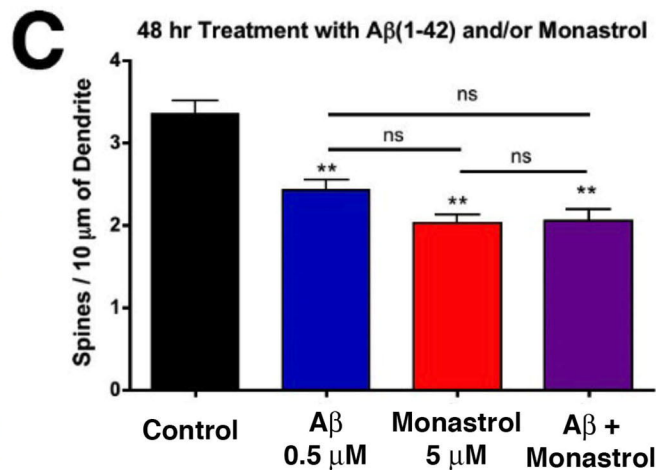
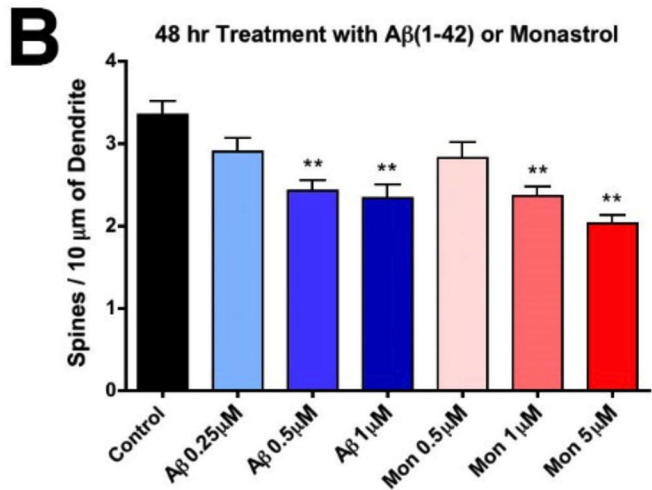
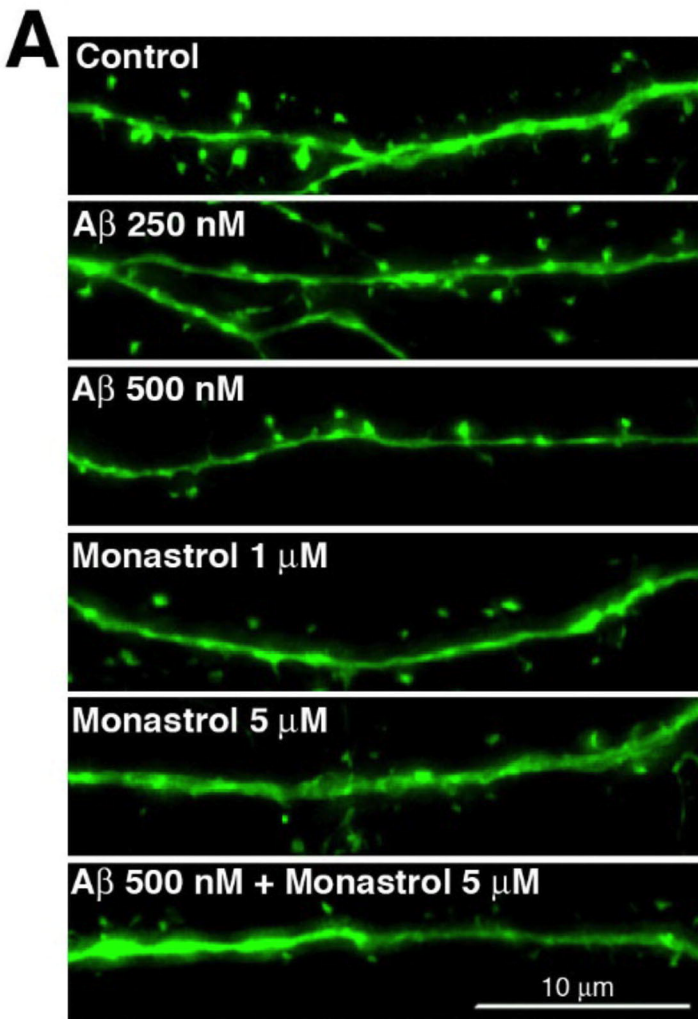


Figure 5